COMSOL
CONFERENCE
2024 FLORENCE

Thermal-Elastohydrodynamic simulation of angular contact ball bearing using COMSOL Multiphysics®

F. Zhang[1], J.-D. Wheeler[2], V. Bruyere[2], J. Raisin[1]
1. TotalEnergies OneTech, Solaize, France
2. SIMTEC, 5 rue Félix Poulat, Grenoble, France

Abstract
Angular contact ball bearings (ACBB) are rolling bearings designed to support both axial and radial loads. The rolling elements (balls in this case) significantly decrease the power losses associated with rotating load bearing by replacing sliding with rolling. However, both the specific kinematic of ACBB and the depth of the ring grooves respectively generate spinning and sliding between the balls and the rings. Together, they contribute to generate frictional power losses.
The specific kinematic of ACBB comes from the axial load the bearing is designed to withstand(1,2): the rotation axes of the rings and the balls are not parallel to each other; this results in spinning induced sliding, and thus, frictional power losses. Moreover, the conformal elliptical contact between the rather deep grooves and the balls creates a large non planar contacting area. Such contact inherently involves sliding apart from the two pure rolling lines. Such sliding also contributes to frictional power losses.
This study investigates the frictional power losses in ACBB by simulating the elliptical contact between a ball and a ring. Under motion, the lubricant fully separates the bodies in elastohydrodynamic lubrication condition. Because of the sliding, the lubricant is sheared which produces heat and activates non-Newtonian effects. An elastohydrodynamic model including both thermal and non-Newtonian effects(3) is used and the kinematic is defined accordingly to the application. Different simulations are run to predict the frictional power losses in the specific ACBB investigated.

Keywords: Thermal-EHD, EHL, Bearing

Introduction
Angular contact ball bearings (ACBB) are widely used in rotating machinery and have gained popularity today due to their low friction and ability to operate at high speeds. They are suitable for applications such as electric motors, aero engines, etc. Nevertheless, the use of ACBB requires an in-depth analysis in order to effectively control the heat generated by the lubricant friction and avoid failures caused by wear.
Many factors contribute to friction in angular contact ball bearings (ACBB), such as rolling friction in the contacts between balls and raceways. A significant factor of friction in ACBBs is produced on the contact ellipses between the balls and the raceways because of the complicated movement of the balls. The kinematic parameters of the balls in an ACBB are complicated and depend on the geometry, the rotational speed of the inner or outer ring and the ball, and the axial and radial loads.
Several theoretical models based on the balance of forces and moments of the balls and the ring have been developed to determine the motions of the balls. The quasi-static model of ball bearings was first proposed by Jones(4). They were reported by Harris(5), Poplawsky(6) and Dominy(7) for high-speed conditions. Depending on the geometry of the balls and the raceways as well as the rotational speed, the forces and contact angles in an ACBB can be evaluated when the motions of the inner ring are known. Therefore, the "raceway control" was adopted, with an "outer raceway control" in high-speed conditions and an "inner raceway control" in low-speed conditions. However, adopting either of these assumptions is difficult and the transition from low to high speed cannot be determined by a distinct relationship.
A more accurate and practical "quasi-dynamic" approach, based on solving the balance of forces, was proposed (8,9). Some researchers then coupled the quasi-dynamic model with thermo-elastohydrodynamic lubrication (TEHL) to study the effects of rotation on the lubricant film thickness and temperature distribution(2,10). However, the quasi-dynamic model does not consider the characteristics of temporal variation of the relative displacement between the bearing components, which limits its transient analysis capabilities.
To develop more complete dynamic models, Walters(11) proposed the dynamic rolling model. The dynamic model obtains the contact force using Hertz's theory and calculates the friction force using a semi-empirical EHD lubrication model. Gupta(12) then expanded the model and developed a first complete dynamic model to solve both the kinematics and dynamics in ball and roller bearings and presented in a later publication a comprehensive manual including his complex software ADORE. In addition, a dynamic rolling simulation tool, called BEAST, was developed by SKF(13). It uses elastohydrodynamic lubrication (EHD) to calculate

the contact force. The traction force was calculated using a non-Newtonian rheological model as a function of the Newtonian film thickness and pressure distributions. However, the dynamic model is more costly compared to the quasi-static and quasi-dynamic models.
In this research, since the operating conditions are considered stationary, the highly accurate and applicable quasi-dynamic model is first adopted. A numerical approach has been developed for angular contact ball bearings inside COMSOL Multiphysics. A thermo-elastohydrodynamic lubrication (TEHL) analysis is performed to evaluate the lubrication state of the elliptical contacts between the ball and the raceway.

Numerical Model

Contact Geometry and Kinematics of Angular Contact Bearings

An angular contact bearing is considered. In this type of bearing, the contact between the balls and the raceways occurs along an axis inclined with respect to the normal plane to the shaft's axis of rotation. This implies that the axis of rotation of the balls is itself inclined with respect to the axis of rotation of the shaft. We focus here on a contact between a ball and the inner and outer rings. Between the ball and race under loading, an elliptical contact area is formed.
The geometrical parameters of the contact have been calculated (1,10,14):

Parameters	Formula	Unit
Bearing inside diameter	d_i	mm
Bearing outside diameter	d_o	mm
Element diameter	D	mm
Contact angle on the inner race	α_i	rad
Pitch diameter	$d_e = (d_i + d_o)/2$	mm
Outer race Curvature	$f_o = r_o/D$	-
Inner race Curvature	$f_i = r_i/D$	-
Radii of curvature of ball (x)	$R_{1x} = \mathrm{D}/2$	mm
Radii of curvature of ball (y)	$R_{1y} = \mathrm{D}/2$	mm
Radii of curvature of inner race (x)	$R_{2x} = \frac{d_e - D\,cos\alpha}{2\,cos\alpha}$	mm
Radii of curvature of inner race (y)	$R_{2y} = -f_i\,D = -r_i$	mm
Reduced radii of curvature (x)	$R_x = \left(\frac{1}{R_{1x}} + \frac{1}{R_{2x}}\right)^{-1}$	mm
Reduced radii of curvature (y)	$R_y = \left(\frac{1}{R_{1y}} + \frac{1}{R_{2y}}\right)^{-1}$	mm
Hertzian contact radius	$R_{ai} = 2Df_i/(2f_i + 1)$	mm
Semi-major axis of the contact ellipse (y)	b	mm

Table 1: Geometrical parameters

The following are the kinematic parameters of an oblique ball bearing, as derived from(1,2,10,15):

Parameters	Formula	Unit
Ball orbital velocity (cage angular velocity)	w_c	rad/s
Ball rotational velocity	w_b	rad/s
Inner race rotational velocity	w_i	rad/s
Outer race rotational velocity	w_o	rad/s
Relative angular speed of inner race	$w_{ri} = w_i - w_c$	rad/s
Ball spinning angular velocity on inner race	$w_{si} = w_{ri}\,sin(\alpha_i)$	rad/s
Distance from the center of the ball to the point on the contact ellipse	$A_i = \left(R_{ai}^2 - y^2\right)^{0.5} - \left(R_{ai}^2 - b^2\right)^{0.5} + ((0.5\,D)^2 - b^2)^{0.5}$	m
Tangential velocity of ball in x direction	$u_{bx} = w_b\,A_i + w_{si}\,y$	m/s
Tangential velocity of inner race in x direction	$u_{ix} = \left(d_e\,/\,2 - A_i\,cos(\alpha_i)\right)w_{ri}$	m/s
Tangential velocity of ball in y direction	$u_{by} = w_{si}\,x$	m/s

Table 2: Kinematic parameters

Generalized Reynolds Equation with Thermal Effects

Because of the sliding prone kinematics, a proper account of the lubricant sheared flow is important. Whilst classical Reynolds equation(16) assumes constant variables across the fluid film, and Navier-Stokes equations are computationally expensive in lubricated contacts(17), generalized Reynolds equation(18) constitutes a recognized solution. The model described below is based on the work of Habchi et al.(3,19,20). Variations of fluid velocity, density, viscosity and temperature across film thickness are acknowledged but integrated before intervening in this generalized Reynolds equation:

$$\boldsymbol{\nabla} \cdot (\bar{\varepsilon}\,\boldsymbol{\nabla} p) - \boldsymbol{\nabla} \cdot \boldsymbol{\rho}^* = 0$$

with p the hydrodynamic pressure, $\bar{\varepsilon} = \frac{\eta_e}{\eta_e'}\rho_e' - \rho_e''$ the new diffusion term gathering cross-film integrated variables detailed in Table 3, and $\boldsymbol{\rho}^* = \left(\rho_x^*\,;\,\rho_y^*\right)$ a density, viscosity and velocity composite convection term with $\rho_i^* = \rho_e'\eta_e\left(u_{t,i} - u_{b,i}\right) - \rho_e u_{b,i}$ its i^{th} component. The velocity of the bottom and top solids in the i^{th} direction are respectively $u_{b,i}$ and $u_{t,i}$. Such framework enables the computation of the fluid velocity in any point in the fluid film:

$$u_{f,i} = \frac{\partial p}{\partial i}\left(\int_0^z \frac{z}{\eta}dz - \frac{\eta_e}{\eta'_e}\int_0^z \frac{1}{\eta}dz\right) + \eta_e\left(u_{t,i} - u_{b,i}\right)\int_0^z \frac{1}{\eta}dz + u_{b,i} \text{ for } i = \{x, y\}$$

Boundary conditions $p = 0$ is applied far enough from the high-pressure region, and the open boundary condition for cavitation is set by applying a penalty term for negative pressures p.

$\rho_e = \int_0^h \rho\, dz$	$\frac{1}{\eta_e} = \int_0^h \frac{1}{\eta}dz$
$\rho'_e = \int_0^h \left(\rho \int_0^z \frac{1}{\eta}dz'\right)dz$	$\frac{1}{\eta'_e} = \int_0^h \frac{z}{\eta}dz$
$\rho''_e = \int_0^h \left(\rho \int_0^z \frac{z'}{\eta}dz'\right)dz$	with h the film thickness, z the coordinate in the direction perpendicular to contact plane, ρ the density and η the viscosity.

Table 3: Integration terms of generalized Reynolds equation

The fluid behavior is defined according to a Tait equation of state (21,22) for temperature and pressure dependence of density, a modified WLF model (23) for temperature and pressure dependence of viscosity and a Carreau-Yasuda-Bair (24) model for shear stress dependence of viscosity. The Tait equation of state relates the lubricant volume V to its volume V_0 at ambient pressure and its volume V_R at reference temperature T_R with the expressions:

$$\frac{V}{V_0} = 1 - \frac{1}{1+K'_0}\ln\left[1 + p\frac{1+K'_0}{K_0}\right]$$
and $$\frac{V_0}{V_R} = 1 + a_v \cdot (T - T_R)$$

with $K_0 = K_{0R}\exp(-\beta_K T)$, $K'_0 = K'_{0R}\exp(\beta'_K T)$, and K_{0R}, β_K, K'_{0R}, β'_K and a_v defined to fit the lubricant behavior. Therefore, the density is expressed relatively to an ambient condition density ρ_R by:

$$\rho(p,T) = \rho_R \cdot \left(\frac{1}{V_0 / V_R} \cdot \frac{1}{V / V_0}\right)$$

The modified WLF expression reads:

$$\mu(p,T) = \mu_G\, exp\left[\frac{-2.303\, C_1\left(T - T_g\right)F}{C_2 + \left(T - T_g\right)F}\right]$$

with $T_g(p) = T_{g0} + A_1\ln(1 + A_2 p)$ the glass transition temperature at a given pressure, T_{g0} the glass transition temperature at ambient pressure, $F(p) = (1 + b_1 p)^{b2}$, and finally μ_G, C_1, C_2, A_1, A_2, b_1 and b_2 defined by regression to fit the lubricant rheology.
Finally, the Carreau-Yasuda-Bair reads:

$$\eta(p,T,\tau) = \frac{\mu(p,T)}{\left[1 + \left(\frac{\tau}{G_{CYB}}\right)^{a_{CYB}}\right]^{\frac{\frac{1}{n_{CYB}}-1}{a_{CYB}}}}$$

with $\tau = \sqrt{\tau_{zx}^2 + \tau_{zy}^2}$ the shear stress norm, τ_{zx}, τ_{zy} its components in the contact plane, and a_{CYB}, n_{CYB} and G_{CYB} defined by regression to fit the lubricant rheology.

The contact load w is balanced by the sum of hydrodynamic pressure p in an ordinary differential equation (ODE) $w = \iint_S p\, dxdy$. This ODE is solved by varying the rigid body distance h_0 between the solids. This distance appears in the film thickness expression:

$$h(x,y) = h_0 + \frac{x^2}{2R_x} + \frac{y^2}{2R_y} + \delta(x,y)$$

with R_x and R_y the reduced curvature radii of the two solids respectively in the direction x and y, and $\delta(x,y)$ is the vertical elastic deformation of the equivalent solid. This equivalent solid is a cubic body which side is large compared to contact dimension. At the cubic body bottom face a fixed boundary condition is applied, on the sides faces, a free condition is applied, and the top is loaded with the contact pressure p.

The variables in Table 3 allow for feeding Reynolds equation with material properties varying across the fluid film because of shear stress variations and temperature differences. Whereas shear stress dependence is described above, the temperature computation requires a heat equation in the fluid film and the solids. The former heat transfer equation reads:

$$\rho C_{pf}\boldsymbol{u_f}\cdot\boldsymbol{\nabla}T - \boldsymbol{\nabla}\cdot\left(k_f\boldsymbol{\nabla}T\right) = Q_{comp} + Q_{shear}$$

with C_{pf} the fluid heat capacity, k_f the fluid heat conductivity, $Q_{comp} = -\frac{T}{\rho}\frac{\partial\rho}{\partial T}\left(\boldsymbol{u_f}\cdot\boldsymbol{\nabla}p\right)$ the compression heat source and $Q_{shear} = \mu\left(\left(\frac{\partial u_{f,x}}{\partial z}\right)^2 + \left(\frac{\partial u_{f,y}}{\partial z}\right)^2\right)$ the shearing heat source. In the solids, the heat equation reads:

$$\rho_j C_{pj}\boldsymbol{u_j}\cdot\boldsymbol{\nabla}T - \boldsymbol{\nabla}\cdot\left(k_j\boldsymbol{\nabla}T\right) = 0 \text{ with } j = \{t, b\}$$

with ρ_j the solid density, C_{pj} its heat capacity and k_j its heat conductivity. The heat equation in the solids and in the fluid film are solved together on a single

solid divided in three domains. More details regarding the domain and the boundary conditions can be found in Habchi's work (3).

Results and discussion

The analysis provides numerical outcomes of the local interactions between the ball and the inner and outer tracks. A sample of the analysis is shown below for the interaction between a ball and the inner track.

The pressure distribution of the contact is illustrated below. The contact is subjected to a high pressure up to several GPa. The film thickness distribution is also obtained on the elliptical contact.

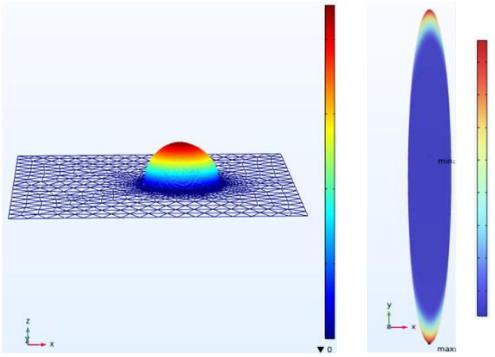

Figure 1: Inner race pressure distribution map [GPa] (left), Inner film thickness distribution (right)

The map of entrainment speed and slip is illustrated as follows. The contact speed field results from a combination of rolling speed, slip and spinning. The slip ratio relative to rolling varies along the *y* axis of the contact.

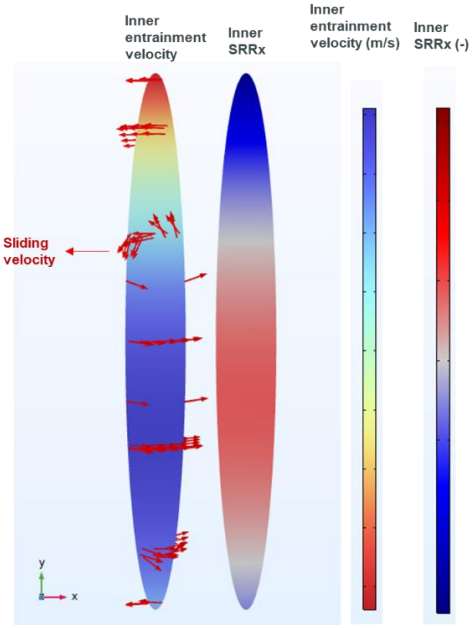

Figure 2: Map of entrainment velocity (left) and slide-to-roll ratio along x direction (SRRx) (Right)

Below is shown the temperature profile, along with the SRR and viscosity. From these results, it is possible to see that heat dissipation by shear is high when slip and viscosity are high, which shows logical consistency.

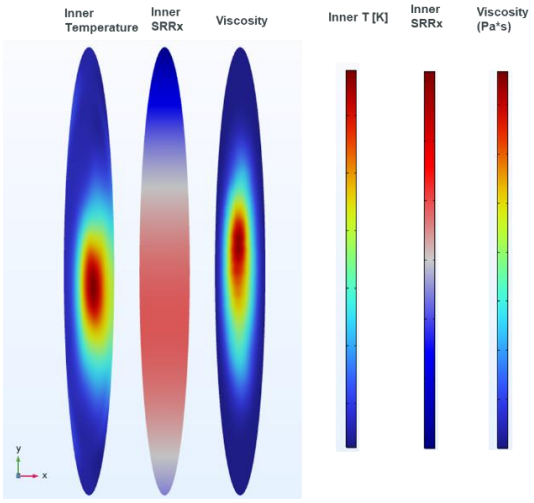

Figure 3: Temperature profile (left), SRRx (middle) and viscosity profiles (right)

Conclusions

This study evaluates the lubrication condition of elliptical ball-race contacts in angular contact ball bearings using a Thermal ElastoHydrodynamic Lubrication (TEHL) analysis. It considers different key operational parameters, such as rotational speed, unloaded contact angle, and external loading. It also gives quantitative results on local contact pressure and temperature profiles, film thickness, velocity and sliding roll ratio (SRR). It can be used to estimate the heat loss from lubricants' friction in angular contact bearings. The numerical approach in this study can predict and optimize lubricant performance in the bearings, especially for thermal aspects and lubrication.

References

1. Popescu A, Houpert L, Olaru DN. Four approaches for calculating power losses in an angular contact ball bearing. Mech Mach Theory [Internet]. 2020 Feb;144:103669. Available from: https://linkinghub.elsevier.com/retrieve/pii/S0094114X19312029
2. Shi X-J, Wang L-Q, Mao Y-Z, Qin F-Q. Coupling study on dynamics and TEHL behavior of high-speed and heavy-load angular contact ball bearing with spinning. Tribol Int [Internet]. 2015 Aug;88:76–84. Available from: https://linkinghub.elsevier.com/retrieve/pii/S0301679X15001012
3. Habchi W. A full-system finite element approach to elastohydrodynamic lubrication problems: application to ultra-low-viscosity fluids [Internet]. Institut National des Sciences Appliquées de Lyon, INSA; 2008. Available from: http://theses.insa-

lyon.fr/publication/2008ISAL0038/these.pdf
4. Jones AB. A General Theory for Elastically Constrained Ball and Radial Roller Bearings Under Arbitrary Load and Speed Conditions. J Basic Eng [Internet]. 1960 Jun 1;82(2):309–20. Available from: https://asmedigitalcollection.asme.org/fluidsengineering/article/82/2/309/442491/A-General-Theory-for-Elastically-Constrained-Ball
5. Harris TA. Ball Motion in Thrust-Loaded, Angular Contact Bearings With Coulomb Friction. J Lubr Technol [Internet]. 1971 Jan 1;93(1):32–8. Available from: https://asmedigitalcollection.asme.org/tribology/article/93/1/32/419027/Ball-Motion-in-ThrustLoaded-Angular-Contact
6. Poplawski J V., Mauriello JA. Skidding in lightly loaded high-speed ball thrust bearings. In: ASME Paper 69-LUBS-20. San Francisco, California; 1969.
7. Dominy J. The Nature of Slip in High-Speed Axially Loaded Ball Bearings. Proc Inst Mech Eng Part C J Mech Eng Sci [Internet]. 1986 Sep 10;200(5):359–65. Available from: http://journals.sagepub.com/doi/10.1243/PIME_PROC_1986_200_139_02
8. Rumbarger JH, Filetti EG, Gubernick D. Gas Turbine Engine Mainshaft Roller Bearing-System Analysis. J Lubr Technol [Internet]. 1973 Oct 1;95(4):401–16. Available from: https://asmedigitalcollection.asme.org/tribology/article/95/4/401/418041/Gas-Turbine-Engine-Mainshaft-Roller-BearingSystem
9. Gentle CR, Pasdari M. Measurement of Cage and Pocket Friction in a Ball Bearing for Use in a Simulation Program. A S L E Trans [Internet]. 1985 Jan 25;28(4):536–41. Available from: http://www.tandfonline.com/doi/abs/10.1080/05698198508981652
10. Yan K, Wang Y, Zhu Y, Hong J, Zhai Q. Investigation on heat dissipation characteristic of ball bearing cage and inside cavity at ultra high rotation speed. Tribol Int [Internet]. 2016 Jan;93:470–81. Available from: https://linkinghub.elsevier.com/retrieve/pii/S0301679X15004326
11. Walters CT. The Dynamics of Ball Bearings. J Lubr Technol [Internet]. 1971 Jan 1;93(1):1–10. Available from: https://asmedigitalcollection.asme.org/tribology/article/93/1/1/419037/The-Dynamics-of-Ball-Bearings
12. Gupta PK. Advanced Dynamics of Rolling Elements. Springer Science & Business Media; 2012.
13. Stacke L-E, Fritzson D. Dynamic behaviour of rolling bearings: Simulations and experiments. Proc Inst Mech Eng Part J J Eng Tribol [Internet]. 2001 Jun 1;215(6):499–508. Available from: http://journals.sagepub.com/doi/10.1243/13506501154375
14. Ricci MC. Ball bearings subjected to a variable eccentric thrust load. In: Dincon'09, 8th Brazilian Conference on Dynamics, Control and Applications. 2009.
15. Rivera G, Tong V-C, Hong S-W. A Study on Ball-Race Contact in Angular Contact Ball Bearing during Rotation. J Korean Soc Precis Eng [Internet]. 2021 Nov 1;38(11):851–62. Available from: http://www.dbpia.co.kr/Journal/ArticleDetail/NODE10621294
16. Reynolds O. On the Theory of Lubrication and its Application to Mr. Beauchamp Tower's Experiments, including an Experimental Determination of the Viscosity of Olive Oil. Trans ASME. 1886;
17. Bruyere V. Une modélisation multi-physique et multi-phasique du contact lubrifié [Internet]. INSA de Lyon; 2012. Available from: https://theses.hal.science/tel-00782322
18. Najji B, Bou-Saïd B, Berthe D. New formulation for lubrication with Non-Newtonian fluids. J Tribol. 1989;111(1):29–34.
19. Habchi W, Eyheramendy D, Bair S, Vergne P, Morales-Espejel GE. Thermal elastohydrodynamic lubrication of point contacts using a Newtonian/generalized Newtonian lubricant. Tribol Lett. 2008;30:41–52.
20. Habchi W, Eyheramendy D, Vergne P, Morales-Espejel GE. A full-system approach to the elastohydrodynamic line/point contact problem. J Tribol. 2008;130(2):21501–10.
21. Hirschfelder JO, Curtiss CF, Bird RB. Molecular Theory of Gases and Liquids. John Wiley & Sons; 1964.
22. Hogenboom DL, Webb W, Dixon JA. Viscosity of Several Liquid Hydrocarbons as a Function of Temperature, Pressure, and Free Volume. J Chem Phys [Internet]. 1967 Apr 1;46(7):2586–98. Available from: https://pubs.aip.org/jcp/article/46/7/2586/211162/Viscosity-of-Several-Liquid-Hydrocarbons-as-a
23. Bair S, Mary C, Bouscharain N, Vergne P. An improved Yasutomi correlation for viscosity at high pressure. Inst Mech Eng. 2012;227:1056–60.
24. Bair S. A Rough Shear-Thinning Correction For EHD Film Thickness. Tribol Trans. 2004;47:361–5.